Ultra-fast Simulation and Inverse Design of Metallic Antennas

Yifei Zheng^{#1}, Constantine Sideris^{#2}

[#]Ming Hsieh Department of Electrical and Computer Engineering, University of Southern California, USA ¹yifeizhe@usc.edu, ²csideris@usc.edu

Abstract — We report a new approach for rapid evaluation and inverse design of metallic antennas. The technique enables electromagnetic solution of candidate antenna structures in less than a second per design without making any approximations, achieving multiple orders of magnitude speedup compared to standard full-wave approaches. The method involves a completely parallelized precomputation stage, which has been GPU-accelerated, used to compute a basis set of numerical Green's functions, which can then be used to reconstruct the field solution for any antenna in the design space by solving an inexpensive linear system. We couple this fast evaluation approach with a directed binary search algorithm and use it to inverse design new, high-gain antennas. We conclude by presenting a practical design of an ultra-wideband planar metallic antenna on ground backed dielectric substrate which achieves 50% fractional bandwidth at a 30 GHz center frequency and greater than 6.8 dB gain across the whole range.

Keywords — antennas, inverse design, computational electromagnetics, numerical methods, optimization.

I. Introduction

Metallic antennas are a very important class of electromagnetic (EM) devices which are responsible for transmitting and receiving information and energy wirelessly. The success of any wireless system crucially depends on the performance characteristics of the antennas used, such as their bandwidth, input impedance, and gain. Unfortunately, except for very basic antennas, analytical solutions do not exist, and new antennas must be designed and evaluated painstakingly using EM simulation software and heuristic approaches. Antennas on dielectric substrates are especially challenging to design due to the propensity for excitation of undesired substrate modes. It is thus no surprise that significant efforts have gone towards developing inverse design methods, which are algorithms for automating antenna design [1]–[5], as well as many other EM devices [6], [7].

Inverse design algorithms for metal antennas can be classified as either gradient-free or gradient-based approaches. Gradient-free approaches include genetic algorithms, particle-swarm optimization, and direct binary search (DBS) [2]–[4]. DBS is particularly well suited for antenna optimization due to the binary nature of metallic antenna design problems. Although these approaches have been shown to be effective for producing high-performance antennas and can naturally handle the discrete nature of the problem, they suffer from requiring many electromagnetic simulations to achieve convergence, often making them impractical for realistic designs. On the other hand, gradient-based approaches parametrize the optimization problem by using a continuously varying set of unknowns,

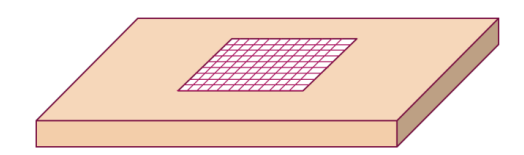


Fig. 1. Example metallic antenna optimization setup on dielectric substrate.

such as the conductivity of the material on the surface [5] or its shape as defined by a levelset [1]. Such approaches are also computationally expensive and often converge to poor local minima or to highly irregular designs with small features which are challenging to fabricate.

In this work, we present a technique which allows the rapid evaluation of any candidate metallic antenna topology in the feasible design space in an arbitrary physical environment and couple it with a DBS optimization algorithm to efficiently inverse high-performance antennas. We consider planar metallic antennas on a finite dielectric substrate, although the approach can be generalized to any configuration for which a discrete parameter design grid can be defined.

II. ANTENNA DESIGN PROBLEM

In order to define an optimization problem, the design space and an objective function must be specified. We define a binary optimization problem with unit cells on a regular Cartesian grid as optimization parameters which can either be empty or filled with metal. Fig. 1 shows an example scenario, in which this grid is located on the top surface of a finite dielectric substrate. The solution space for this problem grows exponentially with the size of the grid—for a grid consisting of $N \times N$ tiles, or N^2 binary variables, this corresponds to $2^{(N*N)}$ possible different antenna designs. Even a coarse 10×10 sized grid admits 2^{100} possible different antennas, making exhaustive search of the design space intractable. Therefore, a heuristic inverse design algorithm must be used to find a design which minimizes or maximizes a desired objective function, such as the antenna bandwidth or pattern. Such optimization algorithms may need hundreds of expensive electromagnetic solutions of candidate designs before converging, which can be very time consuming even on powerful servers. Thus, in order to make such algorithms tractable, we develop a technique which leverages the current-equivalence theorem of Maxwell's equations and reduces the time required to solve any candidate design within the design space by several orders of magnitude, often requiring less than a second per design.

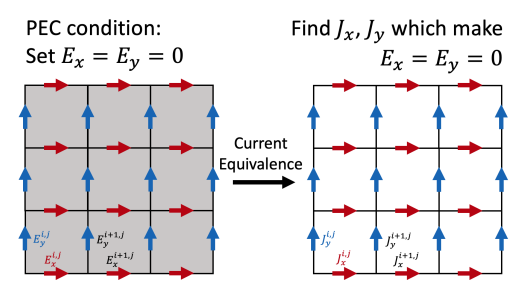


Fig. 2. Depiction of current-equivalence theorem used to represent perfect electrical conductors (PEC) by using equivalent surface current sources.

A. Precomputation

It would be very advantageous if the solution to any antenna design could be constructed by using a linear combination of simulation results, each which have a single metal tile on an otherwise empty grid. If this were possible, we could run N^2 (e.g., 100 for a 10×10 grid) simulations in parallel as a precomputation step and use them to rapidly produce the fields due to any arbitrary design in the $2^{(N*N)}$ design space. Unfortunately, this cannot be done since metals scatter from and interact with each other, thereby prohibiting the use of this simplistic approach to construct the solution to an arbitrary design based on linear combination of the solutions to single-tile designs. However, surface currents, J, unlike metals, do not scatter from each other and satisfy linearity and superposition in Maxwell's equations. Further, it is well known due to the surface-current equivalence theorem that an arbitrary metallic structure can be replaced with an equivalent current distribution, which produces identical electromagnetic fields everywhere in the domain [8]. Fig. 2 demonstrates this equivalence on a 2D Yee cell grid representing a metallic tile. Note that in this work, we use a Yee cell discretization of the fields and sources since we use a Finite-Difference Time-Domain (FDTD) solver to produce electromagnetic solutions; however, any other suitable discretization can be used instead [9]. On the left side of Fig. 2, the metal tile is represented by forcing the tangential E_x and E_y electric field cell components inside it to always remain 0, which enforces the Perfect Electrical Conductor (PEC) condition. On the right side, the PEC condition is enforced instead by finding the sources J_x and J_y inside the region which lead to fields that cancel those produced by the antenna source excitation J_{src} and make the total collocated E_x and E_y field components 0. Thus, any PEC structure can be represented with surface currents $\mathbf{j_{surf}}$ without using material parameters or enforcing the values of the electric fields. These currents can be found by solving the following linear system:

$$G^T Z G \mathbf{j_{surf}} = -G^T \mathbf{e_{src}}, \tag{1}$$

where Z is an impedance matrix mapping each surface \mathbf{J} at the Yee cell level inside the design grid to all of the surface \mathbf{E} field components on the same grid, G is a tall 0-1 selection matrix which selects only the field components corresponding to cells which are inside tiles which should be set to PEC,

 $\mathbf{e_{src}}$ are the surface electric field components inside the whole design grid due to the source at the antenna excitation port, and $\mathbf{j_{src}}$ are the equivalent currents which cancel out the fields on the regions that should be PEC due to the source leading to 0 total tangential E-field. Thus:

$$\mathbf{j_{surf}} = -\left[G^T Z G\right]^{-1} G^T \mathbf{e_{src}},\tag{2}$$

where the G^TZG matrix size depends on the number of Yee cells which are inside tiles that should be set to PEC. This linear system is significantly smaller than the full electromagnetic solution of the antenna, as it only considers the map between the sources inside the planar design region and their corresponding electric field components and does not include any other region in space.

If a direct frequency domain EM solver is used, a single simulation can be used to extract the whole Z matrix. On the other hand, in the case of a time-domain or iterative solver, the impedance matrix Z can be found by performing a sequence of simulations on an empty design grid each with only a single nonzero component in $\mathbf{j_{surf}}$ and recording the resulting fields $\mathbf{e_{surf}}$ over the whole region in each case. Thus, each of these simulations can be used to find a column of Z and if the design grid has been discretized using M Yee cells (counting both x and y components), this will require M total simulations. These simulations can all be run completely in parallel and independently of each other.

The Z matrix mapping from each surface current source to the fields in the domain corresponds to a discrete Green's function for the antenna environment. In rare cases, such as a free-space medium or an infinite layered dielectric substrate, closed-form Green's functions exist and could be used instead. In the present work, we use a custom GPU-accelerated Finite-Difference Time-Domain (FDTD) solver to run the precomputation simulations required to construct the Z matrix. Aside from rapid convergence, the FDTD method additionally allows us to compute the Z matrices for multiple frequencies without additional simulations by using a broadband excitation source and the discrete-time fourier-transform (DTFT). We determined that 3x3 Yee cells (corresponding to 3x4 E_x/J_x and $4x3 E_u/J_u$ cells) is sufficient to accurately discretize a metal tile and therefore 3*4+4*3=12 precomputation simulations are required per tile in the design grid. For each of these simulations, in addition to the surface E-fields in the design region, any other E/H fields in the simulation domain which are needed by the optimization objective function, labeled eh_{opt} are also recorded and stored in a matrix M:

$$\mathbf{eh_{opt}} = M\mathbf{j_{surf}} \tag{3}$$

Once the Z and M matrices have been constructed, the objective function $f_{obj}(\mathbf{eh_{opt}})$ can be rapidly computed for any candidate antenna design by solving for $\mathbf{j_{surf}}$ using (2) and substituting into (3) at each frequency of interest. Note that these are full-wave solutions and no approximations are being made. Since any arbitrary background dielectric or metallic materials can be included in the environment within

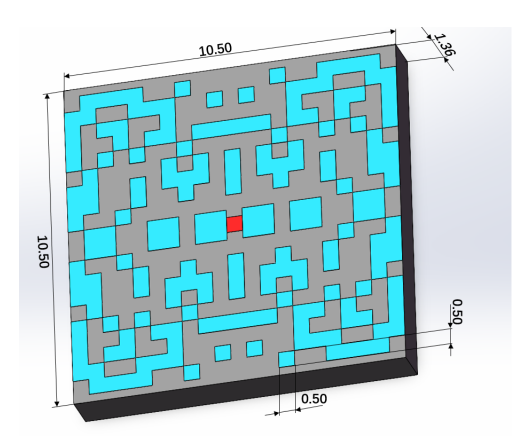


Fig. 3. 3D rendering of the final optimized antenna structure. Dimensions are in millimeters.

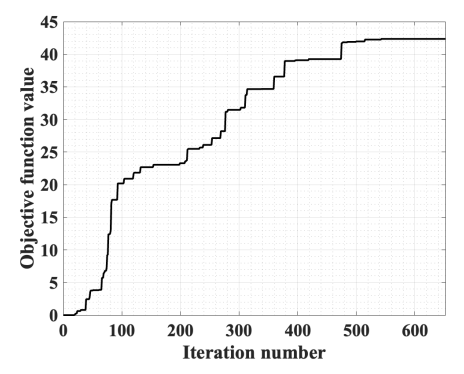


Fig. 4. Plot of objective function (f_{obj}) vs. iteration number history.

the precomputation simulations, and no analytical Green's functions are used, this approach can be used to design any type of antenna, including antennas on finite or layered dielectric substrates.

B. Optimization

We have found that despite its simplicity, the Direct Binary Search (DBS) [4], [10] algorithm works very well to optimize antennas which extremize challenging, nonlinear objective functions. DBS works by choosing a random tile at each iteration and flipping its state from either empty to metal or vice versa. If the flip improves the objective function, it is kept, otherwise it is reverted. The algorithm continues by flipping random tiles and keeping "good" flips until it converges to a local minimum for which no more flips can be made that improve the objective. Due to its random nature, DBS often requires many hundreds of iterations to achieve convergence, making using the rapid evaluation based on precomputation approach described in the prior section a necessity in order to make it feasible. Indeed, the rapid evaluation method enables evaluating any antenna design within the parameter space in less than a second, even on a personal desktop computer.

III. ULTRA-BROADBAND ANTENNA DESIGN EXAMPLE

In order to demonstrate the new methodology, we use it to inverse design a broadband metallic antenna on a ground-backed dielectric substrate. We choose a center frequency of 30 GHz and in order to obtain a broadband result, we also include the performance at 25, 27.5, 32.5, and 35 GHz in our figure-of-merit. We seek to maximize the following nonlinear multi-objective function:

$$f_n = \frac{|S11_n|}{1 + e^{(3 - D_n(0,0))}} + \frac{5 * D_n(0,0)}{1 + e^{(10 - |S11_n|)}}$$
(4)

$$f_{obj} = \frac{1}{\frac{1}{f_1} + \frac{1}{f_2} + \frac{1}{f_3} + \frac{1}{f_4} + \frac{1}{f_5}},\tag{5}$$

where the f_n 's represent the sub-objectives at each frequency n, and $S11_n$ and $D_n(0,0)$ are the S11 in dB and the absolute directivity in the $(\theta=0,\phi=0)$ broadside direction on the far-field sphere at the nth frequency respectively. Note that $S11_n$ and $D_n(0,0)$ can both be computed from $\mathbf{eh_{opt}}$ by evaluating the E-field at the source port location and performing a near-to-far-field transformation respectively. The weighting coefficients for the S11 and the directivity are based on [11] and are designed to increase the relative importance of each objective nonlinearly based on how close they are to achieving the desired performance metrics (in this example, an S11 better than -10 dB and a directivity better than 3). Finally, a harmonic mean is used to combine the sub-objectives f_n into a single scalar objective function f_{obj} that smoothly weights the f_n 's based on the performance at each frequency, emphasizing frequencies which are not performing as well.

A 1.36mm thick Rogers RO3035 ($\epsilon_r = 3.5$) slab is used for the dielectric substrate material with finite 10.5×10.5 mm x/y size. Note that these dimensions correspond to approximately $\lambda \times \lambda \times \lambda/4$ at 30 GHz inside the dielectric. The bottom side of the dielectric is covered by a metal ground reflector. A 50-ohm x-directed lumped port in the center was used as the excitation source. A 21×20 tile optimization grid is used on the top surface, and each tile is discretized using 3x3 Yee cells wherein adjacent tiles share Yee cell components on the shared boundary, resulting in a fine Yee grid of 3786 E_x/J_x and 3780 E_y/J_y components. Due to the XY symmetry of the domain, the number of precomputations required can be reduced by a factor of 4 by precomputing the J_{surf} for one quadrant and using reflections to assemble the other 3, requiring a total of 1892 precomputation simulations. A custom GPU-accelerated FDTD solver is used for the precomputation stage, requiring 38 seconds per simulation. Two simulations were run at each point in time in parallel on a single 36-core Xeon Gold 6154 server each using an Nvidia Titan V GPU. The total time required for the one-time precomputation phase was 10 hours after which evaluating any antenna design within the feasible design space took one second per frequency.

A completely random initial design was chosen to seed the algorithm. Fig. 4 plots the value of the objective function vs. the iteration number. The DBS algorithm took 652 iterations to converge, which at 5 seconds per iteration (due to the 5 frequency points being considered) took 54 minutes total. Note that only the precomputation phase has currently been GPU accelerated and future work seeks to accelerate the prediction algorithm as well. Fig. 3 shows the structure of the final

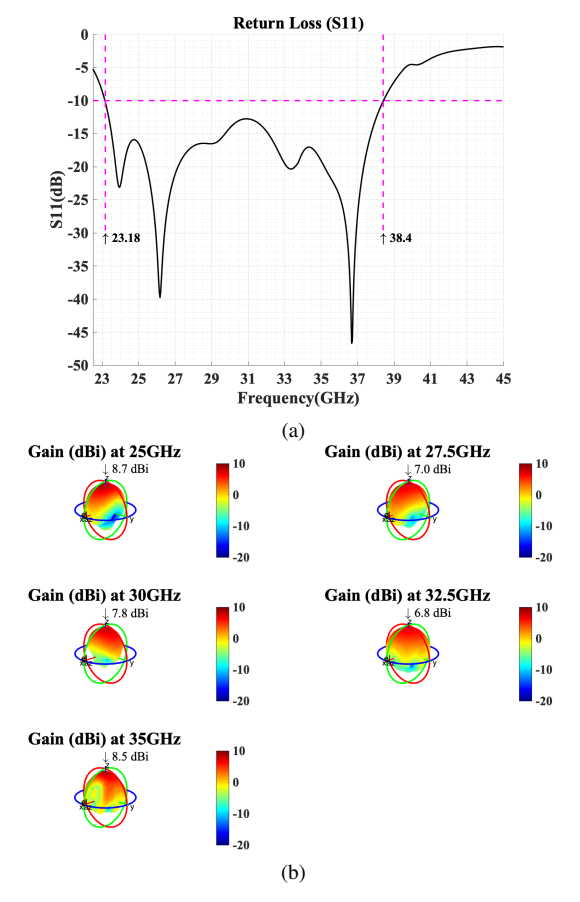


Fig. 5. Antenna performance verified using Ansys HFSS, indicating 50% 10-dB S11 fractional bandwidth and 8.7 dBi peak gain. (a) S11 (dB) vs. frequency, (b) 3D gain patterns (dBi) with peak gain in broadside direction labeled.

optimized design. The final design was simulated in Ansys HFSS to verify its performance, and the S11 and far-field gain patterns at each of the 5 design frequencies are plotted in Fig. 5(a) and (b). The 10-dB S11 bandwidth is 15.2 GHz (23.2 - 38.4 GHz), which corresponds to a 50% fractional bandwidth. The minimum gain across the whole bandwidth is 6.8 dBi at 32.5GHz and the maximum gain is 8.7 dBi at 25 GHz.

IV. CONCLUSION

We have presented an algorithm which enables the rapid evaluation of any feasible metallic antenna design within a designated optimization parameter space by way of a highly parallelized precomputation step. The approach does not use any approximations, computing the exact fields while reducing the time required to evaluate the objective function for inverse designing antennas by several orders of magnitude compared to using a standard EM simulation approach. The potential of the method is demonstrated by using DBS to optimize an ultra-wideband, high-gain dielectric antenna in under one hour of computation time with 50% fractional S11 bandwidth and over 6.8 dBi (peaking at 8.7 dBi) gain across the whole bandwidth in the broadside direction. Future work involves GPU accelerating the optimization phase and fabricating optimized designs for experimental characterization.

ACKNOWLEDGMENT

The authors are grateful for support by the Air Force Office of Scientific Research (FA9550-20-1-0087) and by the National Science Foundation (CCF-2047433, ECCS-2133138).

REFERENCES

- S. Zhou, W. Li, and Q. Li, "Level-set based topology optimization for electromagnetic dipole antenna design," *Journal of Computational Physics*, vol. 229, no. 19, pp. 6915–6930, 2010.
- [2] E. E. Altshuler and D. S. Linden, "Wire-antenna designs using genetic algorithms," *IEEE Antennas and Propagation magazine*, vol. 39, no. 2, pp. 33–43, 1997.
- [3] N. Jin and Y. Rahmat-Samii, "Advances in particle swarm optimization for antenna designs: Real-number, binary, single-objective and multiobjective implementations," *IEEE transactions on antennas and propagation*, vol. 55, no. 3, pp. 556–567, 2007.
- [4] C. Sideris, A. Hajimiri, C. Yang, S.-Y. Wu, F. Sammoura, L. Lin, and E. Alon, "Automated design of a 3d printed waveguide surface coupler," in 2015 IEEE International Symposium on Antennas and Propagation & USNC/URSI National Radio Science Meeting. IEEE, 2015, pp. 318–319.
- [5] E. Hassan, E. Wadbro, and M. Berggren, "Topology optimization of metallic antennas," *IEEE Transactions on Antennas and Propagation*, vol. 62, no. 5, pp. 2488–2500, 2014.
- [6] S. Molesky, Z. Lin, A. Y. Piggott, W. Jin, J. Vucković, and A. W. Rodriguez, "Inverse design in nanophotonics," *Nature Photonics*, vol. 12, no. 11, pp. 659–670, 2018.
- [7] N. Aage, N. Mortensen, and O. Sigmund, "Topology optimization of metallic devices for microwave applications," *International Journal for numerical methods in engineering*, vol. 83, no. 2, pp. 228–248, 2010.
- [8] S. R. Rengarajan and Y. Rahmat-Samii, "The field equivalence principle: Illustration of the establishment of the non-intuitive null fields," *IEEE Antennas and Propagation Magazine*, vol. 42, no. 4, pp. 122–128, 2000.
- [9] A. Taflove, S. C. Hagness, and M. Piket-May, "Computational electromagnetics: the finite-difference time-domain method," *The Electrical Engineering Handbook*, vol. 3, pp. 629–670, 2005.
- [10] B. Shen, P. Wang, R. Polson, and R. Menon, "An integrated-nanophotonics polarization beamsplitter with 2.4× 2.4 μm2 footprint," *Nature Photonics*, vol. 9, no. 6, pp. 378–382, 2015.
- [11] M. R. Khan, C. L. Zekios, S. Bhardwaj, and S. V. Georgakopoulos, "Multi-objective fitness functions with non-linear switching for antenna optimizations," *IEEE Open Journal of Antennas and Propagation*, 2022.